PTPN2 Regulates the Interferon Signaling and Endoplasmic Reticulum Stress Response in Pancreatic β-Cells in Autoimmune Diabetes

Bernat Elvira,[1] Valerie Vandenbempt,[1] Julia Bauzá-Martinez,[2,3] Raphaël Crutzen,[4] Javier Negueruela,[1] Hazem Ibrahim,[5] Matthew L. Winder,[5] Manoja K. Brahma,[1] Beata Vekeriotaite,[1] Pieter-Jan Martens,[6] Sumeet Pal Singh,[7] Fernando Rossello,[8] Pascale Lybaert,[4] Timo Otonkoski,[5] Conny Gysemans,[6] Wei Wu,[2,3] and Esteban N. Gurzov[1]

Diabetes 2022;71:653–668 | https://doi.org/10.2337/db21-0443

Type 1 diabetes (T1D) results from autoimmune destruction of β-cells in the pancreas. Protein tyrosine phosphatases (PTPs) are candidate genes for T1D and play a key role in autoimmune disease development and β-cell dysfunction. Here, we assessed the global protein and individual PTP profiles in the pancreas from nonobese mice with early-onset diabetes (NOD) mice treated with an anti-CD3 monoclonal antibody and interleukin-1 receptor antagonist. The treatment reversed hyperglycemia, and we observed enhanced expression of PTPN2, a PTP family member and T1D candidate gene, and endoplasmic reticulum (ER) chaperones in the pancreatic islets. To address the functional role of PTPN2 in β-cells, we generated PTPN2-deficient human stem cell–derived β-like and EndoC-βH1 cells. Mechanistically, we demonstrated that PTPN2 inactivation in β-cells exacerbates type I and type II interferon signaling networks and the potential progression toward autoimmunity. Moreover, we established the capacity of PTPN2 to positively modulate the Ca^{2+}-dependent unfolded protein response and ER stress outcome in β-cells. Adenovirus-induced overexpression of PTPN2 partially protected from ER stress–induced β-cell death. Our results postulate PTPN2 as a key protective factor in β-cells during inflammation and ER stress in autoimmune diabetes.

Type 1 diabetes (T1D) results from the progressive destruction of insulin-producing β-cells in the pancreatic islets of Langerhans mediated by local infiltration of autoimmune cells, defined as insulitis (1). During early insulitis, inflammation contributes to both the primary induction and secondary amplification of the immune assault resulting in a progressive loss of β-cells (2). The autoimmune process is quite variable between patients and within a particular subject over time (1). The progression of T1D is a nonlinear process, with active and inactive autoimmunity periods in the pancreas, which can last many years. Interestingly, T-cell autoimmunity is negligible in some T1D patients (2). Islet-specific $CD8^+$ T cells constitute a large fraction of the pancreatic $CD8^+$ T cell population also in patients without diabetes (3), and it has been shown that the majority of $CD8^+$ T cells in the T1D pancreas are not islet specific (4). The relevance of the T cell specificity versus nonspecificity in the pancreas is unclear, but it is postulated that the dysfunction

[1]Signal Transduction and Metabolism Laboratory, Laboratoire de Gastroentérologie Expérimental et Endotools, Université Libre de Bruxelles, Brussels, Belgium
[2]Biomolecular Mass Spectrometry and Proteomics, Bijvoet Center for Biomolecular Research and Utrecht Institute for Pharmaceutical Sciences, Utrecht University, Utrecht, the Netherlands
[3]Netherlands Proteomics Centre, Utrecht, the Netherlands
[4]Laboratory of Physiology and Pharmacology, Faculty of Medicine, Université Libre de Bruxelles, Brussels, Belgium
[5]Stem Cells and Metabolism Research Program, Faculty of Medicine, University of Helsinki, Helsinki, Finland
[6]Clinical and Experimental Endocrinology, Department of Chronic Diseases, Metabolism and Ageing, Campus Gasthuisberg O&N 1, KU Leuven, Leuven, Belgium
[7]IRIBHM, Université Libre de Bruxelles, Brussels, Belgium
[8]University of Melbourne Centre for Cancer Research, University of Melbourne, Melbourne, Victoria, Australia

Corresponding author: Esteban N. Gurzov, esteban.gurzov@ulb.be

Received 21 May 2021 and accepted 3 January 2022

This article contains supplementary material online at https://doi.org/10.2337/figshare.17740568.

B.E. and V.V. contributed equally to this work.

C.G. and W.W. contributed equally to this work.

and priming of insulin-producing β-cells can occur via the release of proinflammatory cytokines. Thus, both type I and type II interferon (IFN) signaling are critical for the inflammatory state in invading immune cells and the target β-cells (5,6). Cytokines released during insulitis induce dysfunction in the β-cells and trigger endoplasmic reticulum (ER) stress, contributing to β-cell death (7–9). In addition, ER stress can enhance the induction of posttranslational modifications in islets (10), leading to an increase in deamidation and citrullination of islet autoantigens, which improves the potency to bind HLA molecules and their immunogenic properties.

Protein tyrosine phosphatases (PTPs) are a large superfamily of enzymes that are responsible for the modulation of cellular signaling through dephosphorylation of various tyrosine residues on intracellular proteins (11). All classical PTPs share the same catalytic mechanism with a cysteine residue essential for catalysis, located at the base of the active site (11). The protein tyrosine phosphatase nonreceptor 2 (*PTPN2)* gene encodes PTPN2 (also known as TC-PTP). Results of genome-wide association studies have identified *PTPN2* as a non-MHC risk gene for autoimmunity and linked "loss of function" single nucleotide polymorphisms of PTPN2 with an increased risk of T1D development (12–14). *PTPN2* variants that affect mRNA stability or alter protein structure have also been associated with early-onset T1D (15). Interestingly, the architecture and low thiol pKa of the invariant active site cysteine in the Cys-X_5-Arg motif of PTPN2 renders the protein highly susceptible to oxidation and inactivation by reactive oxygen species, inhibiting the phosphatase activity (11). We have shown that irreversible PTPN2 oxidation occurs in the pancreas from nonobese diabetic (NOD) autoimmune mice (16). Global inactivation of PTPs by oxidative stress enhances IFN signaling in pancreatic islets leading to an increase of proinflammatory chemokine production and exacerbation of STAT1-induced β-cell death (16,17). PTPN2 isoforms are generated by alternative splicing differing in the COOH terminus: a 45 kDa spliced variant contains a nuclear localization sequence and shuttles between the nucleus and the cytoplasm, and a 48 kDa isoform is anchored to the ER (18). Several substrates have been identified for PTPN2 in different cells, including JAK1 and JAK3, Src family, the insulin receptor, and STATs (1,3,5,6). However, the different isoforms and downstream targets by which PTPN2 modulates signaling in β-cells and autoimmune diabetes remain poorly understood.

In the current study, we provide evidence that PTPN2 and ER chaperone expression is increased in the islets of a mouse model of reversed autoimmune diabetes. We report that PTPN2 downregulates the hyperactivation of type I and type II IFN signal transduction and participates in the unfolded protein response in β-cells. Our results shed light on mechanisms that underpin the role of PTPN2 in β-cells in T1D.

RESEARCH DESIGN AND METHODS

Mice

NOD mice, originally obtained from Dr. C.Y. Wu (Peking Union Medical College Hospital, Beijing, People's Republic of China), were housed and inbred in the animal facility of KU Leuven since 1989. The housing of all mice occurred under semibarrier conditions, and animals were fed sterile food and water ad libitum. Mice were screened for the onset of diabetes through evaluation of glucose levels in urine (Diastix Reagent Strips; Bayer, Leverkusen, Germany) and venous blood (Accu-Check; Roche Diagnostics, Vilvoorde, Belgium). Mice were diagnosed as diabetic when they had glucosuria and two consecutive blood glucose measurements >200 mg/dL. Animals were maintained in accordance with the National Institutes of Health *Guide for the Care and Use of Laboratory Animals*, and all experimental procedures were approved and performed following the ethics committees of KU Leuven and by Commission d'Ethique du Bien-être Animal of Université Libre de Bruxelles (reference 732N).

Treatment was initiated on the day of the second high blood glucose measurement, designated as day 0. Hamster anti-mouse CD3 monoclonal antibody (mAb) (clone145-2C11; Bio X Cell, West Lebanon, NH) was administered to mice newly diagnosed with diabetes at a dose of 2.5 μg/mouse i.p. daily for 5 days (19). IL-1RA (Anakinra; Amgen, Thousand Oaks, CA) was administered at a dose of 10 mg/mouse i.p. daily for 5 days. The mice were randomly assigned to treatment groups. Blood glucose values were measured twice weekly, and mice were considered to be in a state of disease reversal if blood glucose measurements were <200 mg/dL. Pancreata were retrieved 33 days after initiation of the therapy. However, when mice did not have disease reversal, they were culled based on human end points: both having dramatic weight loss over a period of <1 week and persistent hyperglycemia with values >600 mg/dL.

Cell Culture and Treatments

Human pancreata were obtained, with informed consent from next-of-kin, from heart-beating, brain-dead donors. Human islets (kindly provided by Professor Piero Marchetti, University of Pisa, Pisa, Italy [clinical characteristics available in Supplementary Table 1]) were isolated in accord with the local ethics committee in Pisa, Italy. After arrival in Brussels, islets were dispersed and cultured as previously described (20). The study was approved by the Erasme Hospital Ethics Committee.

Human Embryonic Stem Cell (hESC) H1 (WiCell, Madison, WI), and the human-induced pluripotent cell (hiPSC) line Hel46.11, derived from human neonatal foreskin fibroblasts and reprogrammed using Sendai virus technology as previously described (21,22), were used in the study. Undifferentiated hiPSC and hESC were cultured on Matrigel-coated (Corning BV, Amsterdam, the Netherlands) plates in E8 medium (Life Technologies, Carlsbad, CA). The cells were differentiated

into β-like cells with use of a 30-day protocol as previously described (23–25) with further modifications (Supplementary Table 2).

The human β-cell line EndoC-βH1 (26) (kindly provided by INNODIA consortium and Dr. R. Scharfmann, University of Paris, Paris, France) was cultured in Matrigel-fibronectin–coated plates.

C57BL/6 mouse islets were washed with cell-dissociation medium and dispersed into single cells with gentle continuous pipetting in trypsin (1 mg/mL; Sigma-Aldrich, St. Louis, MO) and DNase I (1 mg/mL; Sigma-Aldrich) in a water bath at 31°C (27). β-Cells and non-β-cells were purified from dispersed islets through autofluorescence with use of FACS sorting (BD FACSAria III) and lysed with radioimmunoprecipitation assay buffer for immunoblotting.

Cytokine and chemical ER stressor concentrations were selected based on previous time course and dose-response studies (17,28,29 and data not shown). Briefly, cells were cultured with human IFN-γ (1,000 units/mL; PeproTech, London, U.K.), IFN-α (2,000 units/mL; PBL Assay Science, Piscataway, NJ), IL-1β (50 units/mL; R&D Systems, Minneapolis, MN), IL-10 (50 ng/mL; R&D Systems), IL-6 (1,000 units/mL, R&D Systems), IL-17 (1,000 ng/mL; BioLegend, San Diego, CA), IL-21 (1,000 ng/mL; BioLegend), IL-23 (1,000 ng/mL; BioLegend) or TGF-β (1,000 ng/mL; BioLegend). ER stress was induced through adding of sarco/endoplasmic reticulum Ca^{2+}-ATPase (SERCA) blocker(s), thapsigargin (1 μmol/L; Sigma-Aldrich), cyclopiazonic acid (CPA) (75 μmol/L, Sigma-Aldrich), tunicamycin (5 μg/mL; Sigma-Aldrich), or brefeldin A (0.05 μg/mL; Sigma-Aldrich) in medium containing 2% FBS. Vehicle DMSO was added to the control condition in all experiments.

Genome Editing of hESCs

For knockout (KO) of the *PTPN2* gene in H1 hESCs, a pair of CRISPR/Cpf1 (Cas12a) gRNAs was used to remove the identified critical exon 3, which is conserved across annotated protein-coding transcripts. The 23 bp gRNA sequences used to remove exon 3 (protospacer adjacent motif, TTTA 5′-GGATTTGTCTCAACTCTATTATG-3′, and PAM, TTTC 5′-TGACGATGTAATGAATTATGGAC-3′) were designed with use of Benchling Biology Software (2019). The ribonucleoprotein (RNP) components (Alt-R A.s. Cas12a (Cpf1) Ultra and Alt-R A.s. Cas12a crRNA) were purchased from Integrated DNA Technologies (Coralville, IA) and prepared according to the manufacturer protocol. Cells were electroporated with the RNP complexes, and single-cell clones were isolated using limiting dilution. Derived clones were screened by PCR (primers: forward 5′-TGGGCTTTTT CTCCTGGTGT-3′ and reverse 5′-GACGACCAGACACCATC-CAG-3′), and a ∼400 bp deletion of exon 3 in homozygous and heterozygous KO clones was confirmed with Sanger sequencing. Generated clones were karyotyped and characterized for pluripotency with immunocytochemistry and quantitative PCR (qPCR).

Mass Spectrometry, Immunoprecipitation, and Western Blotting

For mass spectrometry analyses, specimens of frozen pancreas were disrupted by beads beating in equal weight of acid-washed glass beads for 10 min at 4°C (30-s on/off cycles). For prevention of experimentally induced oxidation, lysis buffer (10% glycerol, 1% NP-40, 1× complete EDTA-free protease inhibitor cocktail [Roche Diagnostics], 1× phosphatase inhibitor [Sigma-Aldrich]) was degassed with helium for 20 min before use. After tissue disruption, lysed samples were further sonicated for 10 min at 4°C (30-s on/off cycles), and insoluble debris was pelleted at 20,000*g* for 1 h at 4°C. The supernatant was retained for subsequent analysis of total PTP. Chemical derivatization was performed with 10 mmol/L dithiothreitol (DTT) for 1 h. Subsequently hyperoxidation was performed with 1 mmol/L pervanadate for 30 min in the dark. The derivatized tissue lysates were then reduced in 4 mmol/L DTT for 1 h at 20°C and alkylated in 8 mmol/L iodoacetamide for 30 min at 20°C in the dark, for subsequent digestion with Lys-C (1:50) (FUJIFILM Wako Chemicals Europe, Neuss, Germany) for 4 h at 37°C, and then trypsin (1:50) (Sigma-Aldrich) for 16 h at 37°C. Digested tryptic peptides were diluted in PBS for oxidized protein tyrosine phosphatase (oxPTP) pull down. Per sample, 10 μL Protein A/G agarose beads (Santa Cruz Biotechnology, Dallas, TX) was coated with 10 μg oxPTP antibody (R&D Systems) for immunoretrieval of oxPTP peptides. Eluted peptides were cleaned up with homemade strong cation exchange micro-STAGE tips. Liquid chromatography–tandem mass spectrometry analyses of resulting oxPTP peptides were performed as previously described (30). PTPN2 antibody (2 μg) was used for immunoprecipitation, and 50 μL Protein A/G agarose beads (Thermo Fisher Scientific, Waltham, MA) was used for immuno-retrieval of PTPN2-binding proteins.

For Western blotting, cells were lysed with radioimmunoprecipitation assay buffer, and total proteins were extracted and resolved by 12% SDS-PAGE, transferred onto a nitrocellulose membrane, and immunoblotted with antibodies described in Supplementary Table 3 (31). The intensity values of the protein bands were corrected by the values of the housekeeping protein GAPDH, β-actin, or α-tubulin, used as loading controls.

RNA Interference, Adenoviral Transduction, and Cell Viability

We transfected EndoC-βH1 and dispersed human islets with siRNAs or AllStars Negative control siRNA (30 nmol/L; QIAGEN, Venlo, the Netherlands) using Lipofectamine RNAiMAX (Invitrogen, Carlsbad, CA) as previously described (20). siRNA target sequences are provided in Supplementary Table 4.

Adenoviruses carrying green fluorescent protein (GFP) as reporter, a cytomegalovirus promoter, and PTPN2 gene (AdPTPN2) or control (AdControl) were developed by SIRION Biotech (Martinsried, Germany). Virus amplification, purification, titration, and verification were done by SIRION Biotech.

The percentage of viable and apoptotic cells was determined either by inverted fluorescence microscopy with the DNA dyes Hoechst 33342 (20 μg/mL) and propidium iodide (10 μg/mL) (9,32) or by flow cytometry with Zombie Aqua Fixable Viability Kit (1:500; BioLegend) and measured with a BD FACSCanto II cell analyzer (BD Biosciences, San Jose, CA). Viability by fluorescence microscopy was evaluated by at least two independent observers, with one of them unaware of sample identity.

Real-time PCR and RNA Sequencing

Poly(A)+ mRNA extraction was performed with Dynabeads mRNA DIRECT kit (Invitrogen) according to the manufacturer's instructions; reverse transcription was carried out with a reverse transcriptase kit (Eurogentec, Seraing, Belgium). Quantitative real-time PCR was performed with a Bio-Rad CFX machine (Bio-Rad Laboratories, Hercules, CA) and SYBR Green reagent (Bio-Rad Laboratories). β-Actin and/or GAPDH was used as an internal control. Probe and primer details can be found in Supplementary Table 5.

The total RNA was obtained with use of QIAamp DNA Mini Kit (QIAGEN, Hilden, Germany) following the manufacturer's instructions. RNA quality analysis, library preparation, and sequencing were performed by the BRIGHTcore facility (Brussels, Belgium). The sequencing was performed on an Illumina NovaSeq 600. An average of 25 million paired-end reads of 100 nucleotides long were obtained per sample. The list of up-/downregulated genes/transcripts and association with canonical pathways were determined with use of the online Degust software with Limma/Voom and packages Bioconductor EGSEA and ComplexHeatmap in RStudio (Boston, MA). The modulated transcription factors were analyzed withy the online software Predicting ASsociated Transcription factors from Annotated Affinities (PASTAA) with default settings (33). For performance of the rank-rank hypergeometric test, the RRHO and RRHO2 packages were used in RStudio.

Intracellular Calcium Concentration Measurements and Patch-Clamp

EndoC-βH1 cells were transfected with siRNA for 72 h followed by incubation with Fura-2 acetoxymethyl ester (1 μmol/L) for 1 h at 37°C in Krebs solution (115 mmol/L NaCl, 5 mmol/L KCl, 1 mmol/L $CaCl_2$, 1 mmol/L $MgCl_2$, 24 mmol/L $NaHCO_3$, 0.20% BSA, and 10 mmol/L HEPES with pH adjusted to 7.4) supplemented with 0.5 mmol/L glucose. The coverslips were then transferred to a tissue chamber filled with Krebs solution supplemented with 1 mmol/L glucose and mounted on an inverted fluorescence microscope (Diaphot TMD; Nikon, Tokyo, Japan) for epifluorescence. Fura-2 fluorescence of single cells was measured with dual-excitation fluorimetry with use of a camera-based image analysis system (MagiCal; Applied Imaging, Sunderland, UK). The excitation and emission wavelengths were set at 340/380 and 510 nm, respectively, and pair images (at excitations of 340 and 380 nm, 30-ms interval) were taken every 2.5 s. Intracellular Ca^{2+} concentration was calculated from the ratios of the 340- and 380-nm signals as previously described with MetaFluor software (Molecular Devices, San Jose, CA) (9,34).

Patch-clamp of differentiated H1 PTPN2 KO and control aggregates was conducted as previously described (35). For voltage measurements, gramicidin-perforated whole-cell configuration patch-clamp experiments were conducted. Bath solution contained the following: 110 mmol/L NaCl, 10 mmol/L HEPES, 4 mmol/L KCl, 1 mmol/L $MgCl_2$, 1 mmol/L $CaCl_2$, and 24 mmol/L $NaHCO_3$, pH 7.4, with NaOH supplemented with 2.8 or 20 mmol/L D-glucose, osmolarity 299 or 319 mOsmol/L. Pipette solution contained 10 mmol/L NaCl, 20 mmol/L KCl, 24 mmol/L K_2SO_4, 90 mmol/L KCl, 25.9 mmol/L D-mannitol, and 5 mmol/L HEPES, pH 7.2, with KOH, supplemented with 50–150 ng/mL gramicidin, osmolarity 304 mOsmol/L. Stock solution of gramicidin (5 mg/mL in DMSO) was daily prepared. Filled pipettes had resistances of 8–10 MΩ. Whole-cell configuration induced by gramicidin permeabilization was achieved within 15–20 min. Leak resistance after sealing >1.5 GΩ and access resistance <35 MΩ were required to allow the recordings. Aggregates were stored in an incubator and used within 1 h of incubation in the patch-clamp chamber. Voltages were monitored with a HEKA EPC 10 amplifier (HEKA Elektronik, Lamprecht, Germany). Zero-current whole-cell voltages were continuously recorded with use of PATCHMASTER software (HEKA Elektronik).

Immunofluorescence

Cells were fixed with 4% paraformaldehyde (Sigma-Aldrich), permeabilized with 0.5% Triton X-100 (Sigma-Aldrich) and unspecific binding sites blocked with Ultravision Protein Block (Thermo Fisher Scientific). Cells were then incubated with primary antibodies overnight at 4°C followed by 1-h incubation with the secondary antibody conjugated to the fluorochrome (Supplementary Table 3). Next, cells were mounted with use of VECTASHIELD Antifade Medium Mounting with DAPI (Sigma-Aldrich).

Mouse pancreata were fixed with formalin and embedded in paraffin. Sections (5–10 μm) were dewaxed, and antigen unmasking was performed with heated sodium citrate buffer. Sections were permeabilized with 0.1% Triton X-100, and unspecific binding sites were blocked with 5% normal goat or donkey serum (Sigma-Aldrich) according to the host of the secondary antibody for 1 h at room temperature. After blocking, sections were incubated with primary antibodies as described in Supplementary Table 3 and then incubated with Alexa Fluor (Thermo Fisher Scientific) secondary antibodies except for BiP/GRP78 Alexa Fluor 488 and counterstained with DAPI (1 μg/mL; Sigma-Aldrich).

Images were analyzed on Axio Imager Z1 microscope using ZEISS ZEN blue software (Carl Zeiss AG, Oberkochen, Germany). The fluorescence intensity quantification within

the murine pancreas section was analyzed with CellProfiler software (Broad Institute, Cambridge, MA).

Statistical Analysis

The results are presented as the mean ± SEM. Student *t* test was used for comparisons between two groups. Differences among groups were assessed with two-way ANOVA or repeated-measures ANOVA. Statistical analyses were assessed with Graphpad Prism software (GraphPad Software 8, La Jolla, CA). Sample size was predetermined based on the variability observed in prior experiments and on preliminary data. Differences were regarded as statistically significant if $*P < 0.05$, $**P < 0.01$, or $***P < 0.001$.

Data and Resource Availability

The RNA-sequencing (RNA-Seq) data set generated during the sequencing procedure is deposited in the Gene Expression Omnibus (GEO) database (access no. GSE172148), and the mass spectrometry proteomics and peptidomics data have been deposited to the ProteomeXchange Consortium via PRIDE (access no. PXD025394) and are available from the corresponding author on reasonable request.

RESULTS

Proteomic Screening Identifies Increased Pancreatic Chaperones and PTPN2 Expression in NOD Mice With Diabetes Remission After Anti-CD3 + IL-1RA Treatment

To identify anti-inflammatory targets in NOD mice with reversed hyperglycemia, we took advantage of non-Fc receptor (FcR) binding anti-CD3 mAb and IL-1RA treatment to preserve insulin production (36) and assessed protein expression and PTP profile in the pancreas. We confirmed that administration of anti-CD3 + IL-1RA in a small cohort of hyperglycemic mice significantly reversed diabetes, compared with a low dose of anti-CD3 alone used as control (not cured, Fig. 1*A*). We isolated snap-frozen pancreas from treated NOD mice and performed a mass spectrometry analysis, as previously described (30,31). Samples were divided for detection of the global protein profile, PTP spectral counts, and individual PTPs (Supplementary Fig. 1*A*). We detected 1,452 proteins; from those, 117 upregulated and 8 downregulated proteins were significantly modulated in the anti-CD3 + IL-1RA group compared with the controls (Fig. 1*B*). Pathway analysis showed that ER stress response and protein folding are at the top of the significantly modulated pathways in the cured mice (Fig. 1*C*). We observed increased expression of the chaperones BiP, GRP94, Hsph1, and Erp44 and chaperone/associated protein MANF (Fig. 1*D*). In addition, we observed protein modulation of eukaryotic initiator factors and the oxidative stress response in the pancreas from anti-CD3 + IL-1RA–treated mice (Supplementary Fig. 1*B*). Anti-CD3 + IL-1RA therapy impacts proinflammatory cytokine signaling (36). For identification of tyrosine phosphatase expression, all PTPs were reduced in the sample by treatment with DTT, followed by hyperoxidation using pervanadate, which converts all catalytic cysteines of PTPs into the sulphonic acid (SO_3H) state, allowing detection of phosphatases by immunoprecipitation with an oxPTP antibody binding to the majority of classical PTPs (Supplementary Fig. 1*A*). Of 17 PTP motif peptides detected (Supplementary Fig. 1*C*), 2 were found significantly regulated in NOD mice with reversed diabetes, namely, PTPN2 was increased and PTPN13 decreased compared with controls (Fig. 1*E*). *PTPN2* is a candidate gene for T1D development, and PTPN13 (Fap-1) is a negative regulator of apoptotic cell death induced by Fas (37). PTPN2 is expressed in FACS-purified β-cells, non-β-cells, and acinar cells from C57BL/6 mice (Fig. 1*F*). Interestingly, NOD islets showed lower levels of PTPN2 compared with C57BL/6 islets (Fig. 1*G*). We observed a low expression of PTPN2 in immune infiltrated islets from noncured control, anti-CD3–treated, and anti–IL-1RA–treated mice (Fig. 1*H* and Supplementary Figs. 2 and 3). Conversely, PTPN2 is highly expressed in insulin-positive cells and also detected in surrounding immune cells (insulitis) in the anti-CD3 + IL-1RA–treated mice (Fig. 1*H* and Supplementary Figs. 2 and 3). Moreover, PTPN2, BiP, GRP94, and MANF positively correlated with insulin in the islets (Fig. 1*H* and *I* and Supplementary Figs. 4–6). IL-1β treatment did not affect PTPN2 expression in mouse islets, EndoC-βH1 cells, or β-like cells (Supplementary Fig. 7*A*–*C*). It was previously shown that the combination therapy induced immune regulatory mechanisms (36), including increased $Foxp3^+$ splenic Tregs and IL-10 production. We observed that IL-10 + IFN-γ (induced by anti-CD3) significantly upregulated PTPN2 expression in EndoC-βH1 cells (Fig. 1*J*). We concluded that the unfolded protein response and PTPN2 in β-cells/islets positively correlates with β-cell survival in the anti-CD3 + IL-1RA–treated NOD mice.

PTPN2 Modulates the IFN-γ–Mediated Inflammatory Response Through STAT1 Phosphorylation in Human β-Like and EndoC-βH1 Cells

To gain mechanistic insight into the role of PTPN2 in pancreatic β-cells, we first took advantage of a well-established seven-stage differentiation protocol to evaluate the expression of PTPN2 in differentiated β-like cells. OCT4, SOX17, PDX1, NKX6.1, glucagon, and insulin have been used as differentiation markers (Fig. 2*A* and Supplementary Fig. 8*A*). We achieved an average of 30–40% efficiency of insulin-positive cells (Fig. 2*B* and Supplementary Fig. 8*B*). Interestingly, PTPN2 protein expression was significantly decreased from stage 4 in the β-like cell differentiation of both Hel46.11 and H1 stem cells (Fig. 2*C* and data not shown). We knocked out PTPN2 using CRISPR/Cpf1 deletion of exon 3 in H1 cells (Fig. 2*D* and Supplementary Fig. 9*A*–*D*). Both PTPN2 KO and control H1 hESC were differentiated into insulin-producing β-like cells (Supplementary Fig. 9*E*). To mimic the β-cell response to a localized autoimmune attack, we pulsed differentiated β-like cells with 1-h exposure of IFN-γ followed by a washout of the cytokine and subsequent analysis of activated

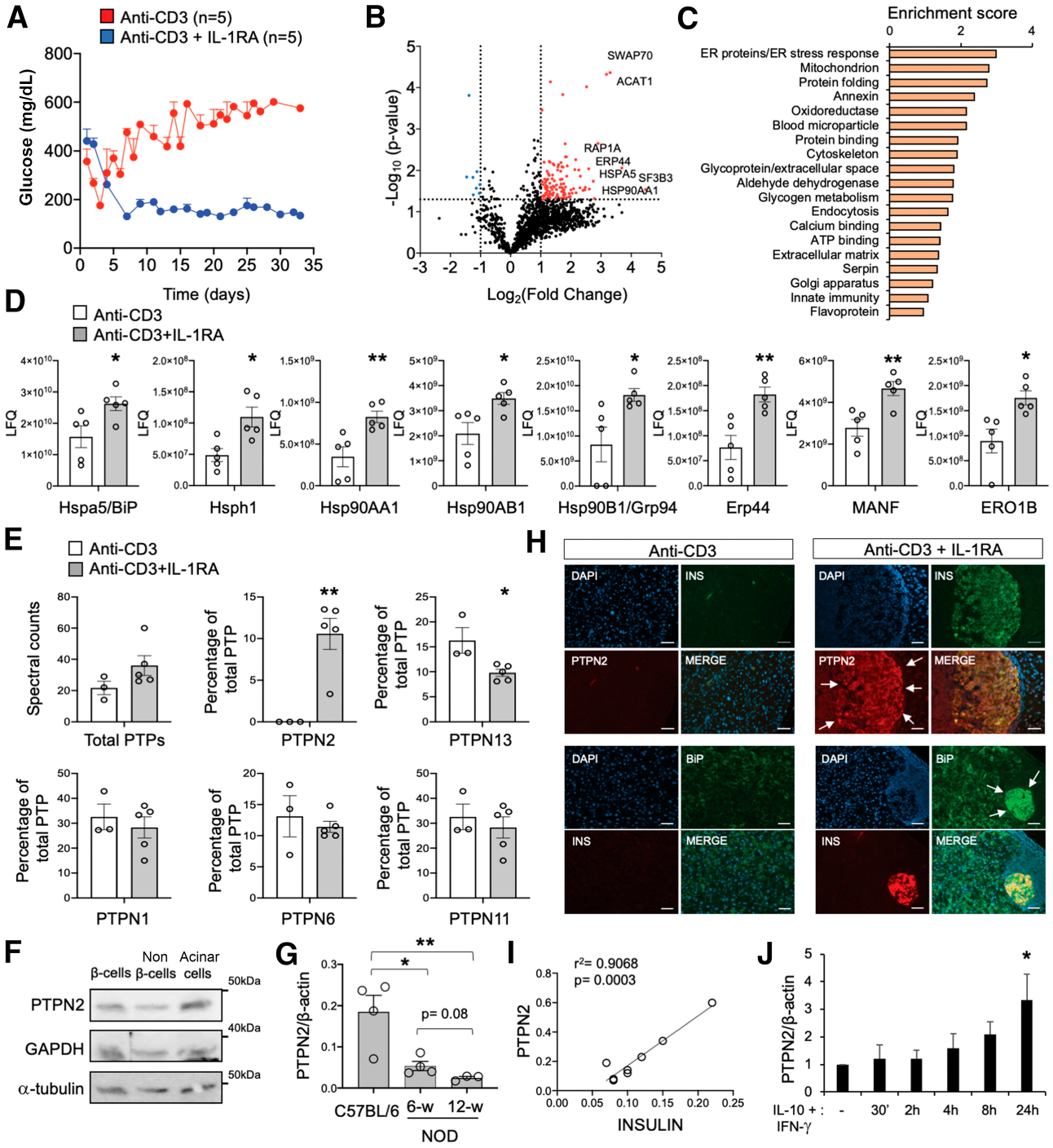

Figure 1—Treatment with anti-CD3 + IL-1RA reversed diabetes in newly diagnosed diabetic NOD mice with an increase of protein levels of PTPN2 and chaperons in pancreatic islets. *A*: Newly diagnosed diabetic NOD mice were treated with anti-CD3 mAb + IL-1RA or anti-CD3 as control. Murine blood glucose was examined by glucometer two times weekly for 33 days. $n = 5$. *B*: Volcano plots of upregulated (red) or downregulated (blue) proteins in the mass spectrometry analysis. $n = 5$. *C*: Enriched pathway analysis of combined anti-CD3 + IL-1RA treatment or anti-CD3 control pancreas. Only pathways with $P < 0.05$ are shown. *D*: Protein profile of pancreata was examined by mass spectrometry. Protein expression of ER stress response–related proteins is shown. LFQ, label-free quantification. $n = 5$. *E*: Protein expression of PTPs in anti-CD3 + IL-1RA or control pancreas examined by mass spectrometry. $n = 3$–5. *F*: Expression of PTPN2 was determined in FACS-purified β-cells, non-β-cells, and acinar cells. Western blot representative of two independent experiments. *G*: Islets were isolated from 12-week-old C57BL/6 and 6- and 12-week-old NOD mice. Gene expression of PTPN2 and β-actin was examined by qPCR. $n = 3$–4. *H*: Immunofluorescence analysis of insulin and BiP or PTPN2 in pancreas sections. The nuclei were visualized with DAPI. PTPN2 or BiP and insulin-positive cells are shown (white arrows). Scale bar: 50 μm. *I*: Insulin and PTPN2 correlation in pancreatic islets from anti-CD3 + IL-1RA treatment is shown. *J*: EndoC-βH1 cells were treated with IL-10 + IFN-γ as indicated. PTPN2 and β-actin were assessed by qPCR. $n = 4$. $^*P < 0.05$; $^{**}P < 0.01$.

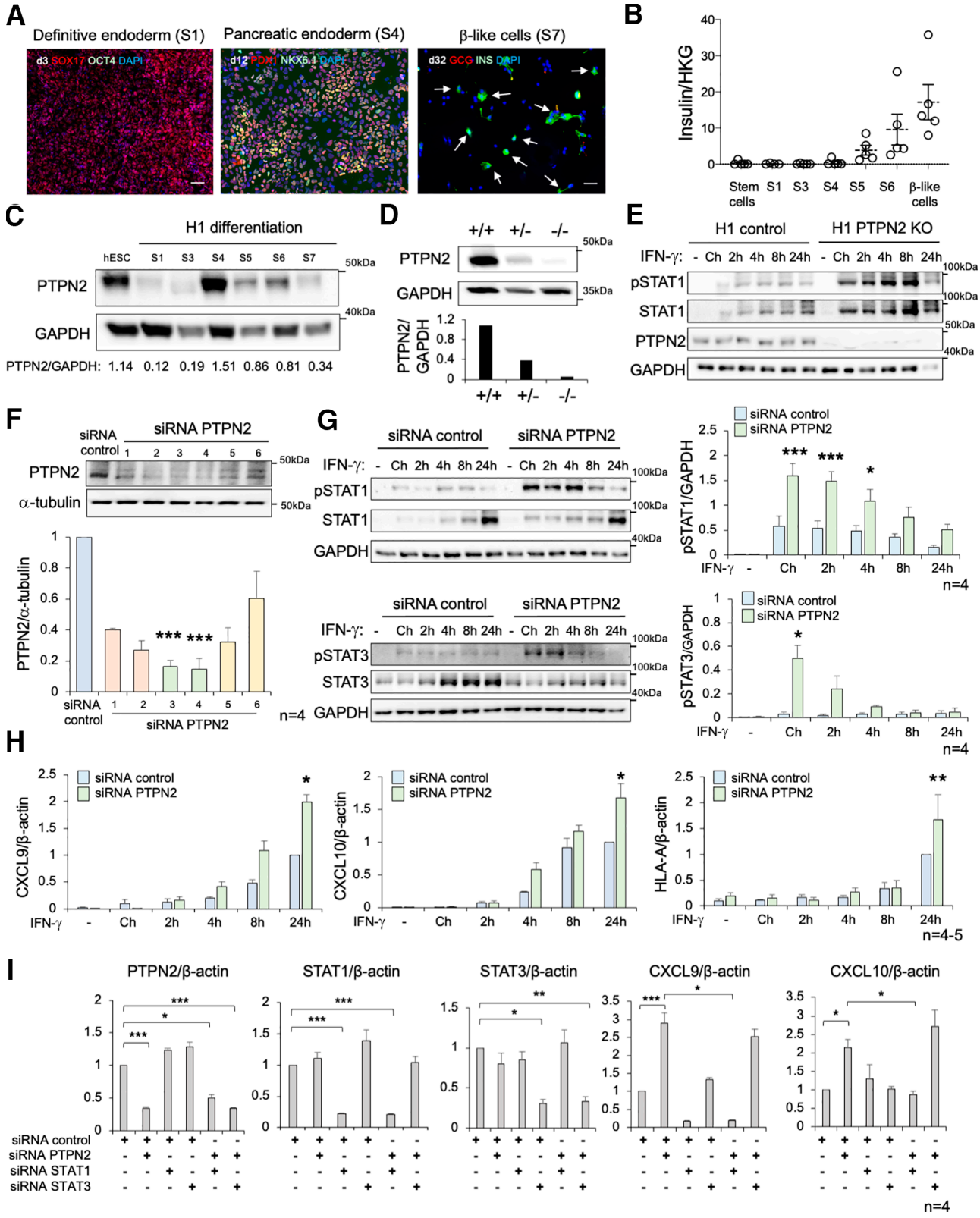

Figure 2—PTPN2 regulates IFN-γ signaling in pancreatic β-cells. *A*: Immunofluorescence staining of Hel46.11 hiPSC differentiation markers in the different stages as indicated. Insulin-positive cells are shown (white arrows). Scale bar: 50 μm. *B*: Insulin mRNA expression was assessed with real-time PCR in the different stages of Hel46.11 hiPSC differentiation into β-like cells. Results were normalized with the mean of GAPDH and β-actin as internal housekeeping genes (HKG). $n = 5$. *C*: Western blot for PTPN2 expression in H1 hESC differentiation into β-like cells. The relative protein expression of the PTPN2 shown was quantified by dividing the intensity values against GAPDH as internal housekeeping protein with use of ImageJ software. *D*: Western blot for PTPN2 was performed in undifferentiated H1 hESC cells

signaling at different time points (chase). We first focused on STAT1, an IFN-induced transcription factor that has been implicated in β-cell dysfunction and death (17,38). *PTPN2* deletion by CRISPR/Cpf1 prolonged the chase activation of STAT1 by phosphorylation after a 1-h pulse of IFN-γ in β-like cells (Fig. 2*E*).

Stem cell differentiation produces a mix of hormone-expressing endocrine-like cells. To study PTPN2-modulated signaling specifically in human insulin-producing β-cells, we took advantage of EndoC-βH1 cells and siRNA technology. We selected the siRNAs with higher PTPN2 knockdown efficiency (nos. 3 and 4) from the six different siRNAs tested (Fig. 2*F*). Cells were transfected with siRNA PTPN2 (no. 4 unless otherwise indicated), treated with IFN-γ in a 1-h pulse and chase experiment, and the effect of PTPN2 knockdown on the kinetics and magnitude of IFN-γ–induced STAT1 and STAT3 phosphorylation was evaluated. The IFN-γ–mediated phosphorylation of STAT1/3 proteins occurred with different kinetics in the EndoC-βH1 cells, but it was markedly prolonged in cells in which PTPN2 was knocked down (Fig. 2*G* and Supplementary Fig. 10).

Given that PTPN2 deficiency enhanced STAT activity, we next asked whether the downstream gene targets are affected. In keeping with previous studies (17,38), we observed increased CXCL9, CXCL10, and HLA/MHC class I activation in PTPN2 knocked down cells (Fig. 2*H*). Both STAT1 and STAT3 are phosphorylated on tyrosine residues, forming dimers through the reciprocal SH2 domain/phosphotyrosine interactions and binding to γ-activated sequence elements. However, STAT1 and STAT3 dimers selectively bind to similar but not identical elements (39). To assess the transcription factor responsible for chemokine expression in PTPN2-inhibited cells, we silenced PTPN2 and STAT1 or STAT3 in a double-knockdown approach (Fig. 2*I*). As previously shown, inhibition of PTPN2 significantly exacerbated CXCL9 and CXCL10 expression 24 h after the pulse with IFN-γ. This effect was abrogated by STAT1 but not STAT3 knockdown (Fig. 2*I*), suggesting that STAT1 is the main inflammatory enhancer driving chemokine expression in IFN-γ–treated PTPN2-deficient β-cells.

Inactivation of PTPN2 Increases and Prolongs Type I and Type II IFN Signaling in β-Cells

Elevated levels of type I IFN were found exclusively in the pancreas and islets from T1D patients (6,40) and have been associated with the early stages of the development of autoimmune diabetes in humans (41) and rodents (42). We performed a 1-h IFN-α pulse and chase experiment in PTPN2-deficient β-like and EndoC-βH1 cells. Similar to IFN-γ–treated cells, PTPN2 inactivation increased STAT1 phosphorylation (Fig. 3*A* and *B*). PTPN2-mediated STAT1 hyperactivation was markedly prolonged after the pulse of IFN-γ (Fig. 2*D*) compared with IFN-α (Fig. 3*A*). Similar results were observed between PTPN2-deficient β-like and EndoC-βH1 cells treated with IFN-γ or IFN-α (Figs. 2*F* and 3*B*). Next, we performed RNA-Seq analysis of type I and type II IFN-treated PTPN2-deficient and control EndoC-βH1 cells to determine the comprehensive footprint induced 24 h after the 1-h exposure to the different cytokines. First, we validated the PTPN2 knockdown efficiency, insulin levels, and STAT1-modulated gene expression in the samples (Fig. 3*C*). No differences were observed in glucose-stimulated insulin secretion after PTPN2 knockdown in EndoC-βH1 cells (Supplementary Fig. 11). As expected, STAT1 targets SOCS1, CXCL9, CXCL10, and CXCL11 were upregulated in PTPN2-deficient IFN-γ–treated EndoC-βH1 cells (Fig. 3*C*). Profiling of the data set using the Gene Ontology (GO) method for gene set testing allowed us to identify several modulated pathways by PTPN2 silencing including the unfolded protein response (Fig. 3*D*). To refine the potential list of PTPN2 target genes, we analyzed the top upregulated and downregulated genes and pathways affected by control and type I and type II IFN–treated cells (Fig. 3*E* and Supplementary Figs. 12 and 13). Knockdown of PTPN2 upregulated T1D-related pathways: antigen processing and presentation via MHC class I, antigen processing and presentation of peptide antigen, and response to IFN (Supplementary Fig. 12). In addition, PTPN2 deficiency significantly increased the persistent activation of gene expression induced by the proinflammatory cytokines (Fig. 3*F* and *G*).

To identify transcription factors responsible for gene network modulation by PTPN2, we used the PASTAA software (33) (Fig. 4*A*). The signature of transcription factors SP1, STAT, IRF, and NF-κB responsible for immune signaling in β-cells (29,43) was increased after PTPN2 knockdown and IFN-γ treatment. We observed enhanced degradation of IκBα, a repressor of NF-κB, in IFN-γ–treated PTPN2 knockdown cells (Fig. 4*B*). NF-Y, associated with MHC gene expression (44), was found to be at the top of the PTPN2-modulated transcription factor in IFN-α–treated cells (Fig. 4*A*). We performed a Rank-Rank Hypergeometric Overlap (RRHO) analysis (45), comparing ranked lists of genes identified with RNA-Seq of primary β-cells of individuals affected by T1D (46) and our data set. There is a low or no correlation between EndoC-βH1

with CRISPR/Cpf1 deletion of *PTPN2*: H1 wild type (+/+), H1 heterozygous KO (+/−), and H1 homozygous KO (−/−). Western blot is representative of two independent experiments. *E*: hESC-derived β-like cells (H1 control and H1 homozygous PTPN2 KO [H1 PTPN2 KO]) were cultured with 1-h pulse of IFN-γ followed by a change of the media and starting of the chase (Ch) measures at the indicated time points. Western blot for phosphorylated (p)STAT1, total STAT1, and PTPN2 was performed. $n = 4$. *F*: EndoC-βH1 cells were transfected with control or six different PTPN2 siRNAs. $n = 4$. *G*: Transfected cells with control or PTPN2 siRNA were cultured with IFN-γ for 1 h in a pulse-chase experiment. Western blot for phosphorylated STAT1/3 and total STAT1/3 was performed. $n = 4$. *H*: Transfected cells with control or PTPN2 siRNA were cultured with IFN-γ for 1 h in a pulse-chase experiment. Gene expression was examined by qPCR. $n = 4$–5. *I*: Transfected cells with control or double transfection with PTPN2, STAT1, or STAT3 siRNA were cultured with IFN-γ for 1 h. Gene expression of PTPN2, STAT1, STAT3, and chemokines was examined with qPCR 24 h after cytokine treatment. $n = 4$. $^*P < 0.05$; $^{**}P < 0.01$; $^{***}P < 0.001$.

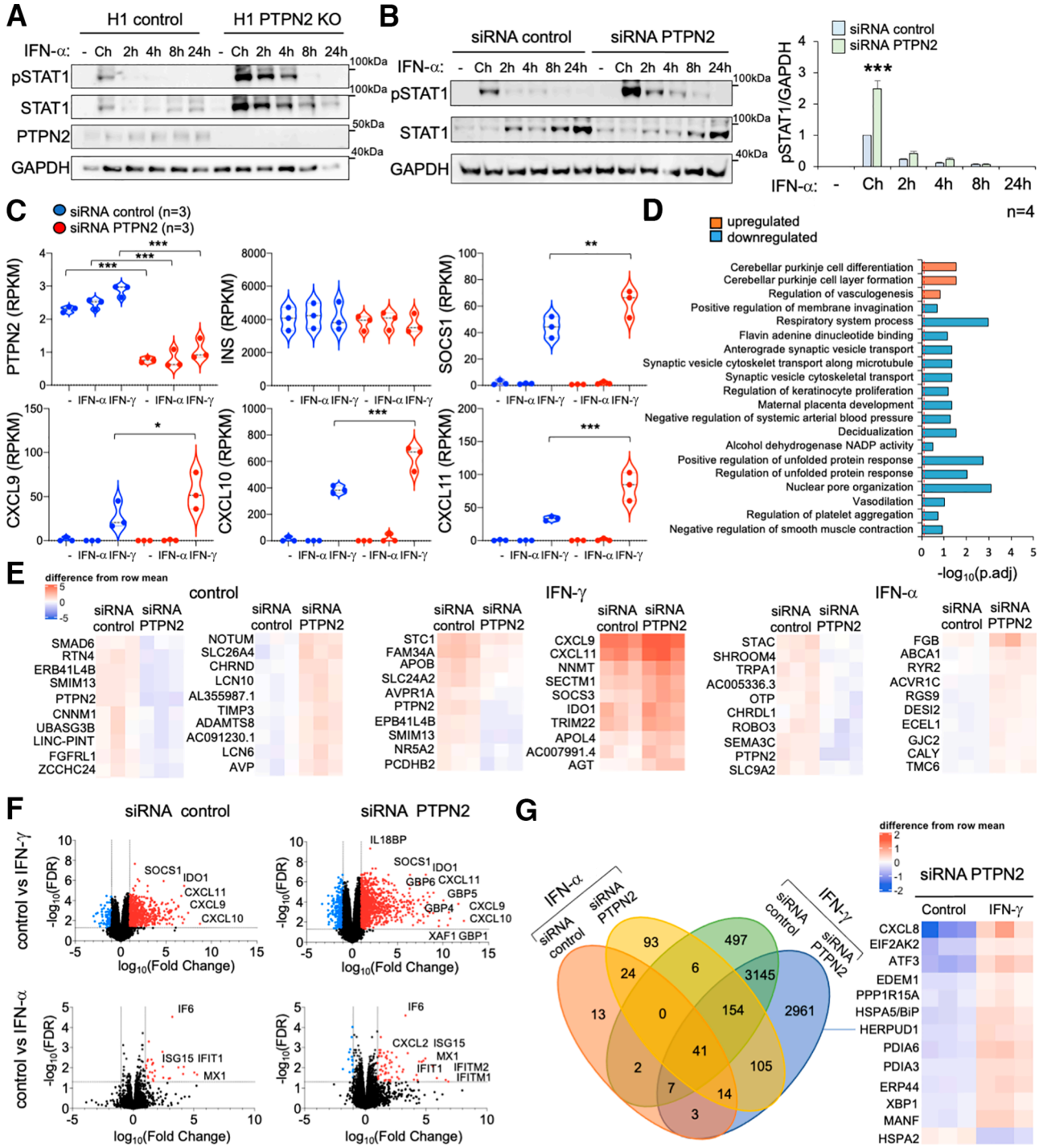

Figure 3— PTPN2 is a master regulator of type I and type II IFN–associated pathways in β-cells. *A*: hESC-derived β-like cells were cultured with 1-h pulse of the proinflammatory cytokine IFN-α followed by a change of the media and starting of the chase (Ch) measures at the indicated times. Western blot for phosphorylated (p)STAT1, total STAT1, and PTPN2 was performed. Western blot representative of three independent experiments. *B*: Transfected EndoC-βH1 cells with control or PTPN2 siRNA were cultured with IFN-α for 1 h in a pulse-chase experiment. $n = 4$. *C*: Gene counts obtained by RNA-Seq were normalized to reads per kilobase million (RPKM) with RStudio. $n = 3$. *D*: Pathway enrichment analysis of the comparison between siRNA PTPN2 or control transfected EndoC-βH1 cells obtained with RNA-Seq. Length of bars is proportional to the level of significant change, expressed by the negative logarithm of the adjusted *P* value. Pathways are considered significantly modulated upon $-\log_{10}(P_{adjusted}) > 1.3$. *E*: The top 10 most significant up- or downregulated genes in the RNA-Seq data set are visualized with heat maps, and the counts are scaled to the difference of the row mean. Gene expression is considered significant upon false discovery rate (FDR) <0.05. $n = 3$. *F*: Volcano plots of upregulated (red) or downregulated (blue) genes in the RNA-Seq data set as indicated. Genes are considered significantly modulated upon log fold change > 1 and $-\log_{10}$(false discovery rate) > 1.3. *G*: The Venn diagram represents the overlap of genes modulated in the different groups. Gene expression is considered significant upon a false discovery rate <0.05. $n = 3$. *$P < 0.05$; **$P < 0.01$; ***$P < 0.001$.

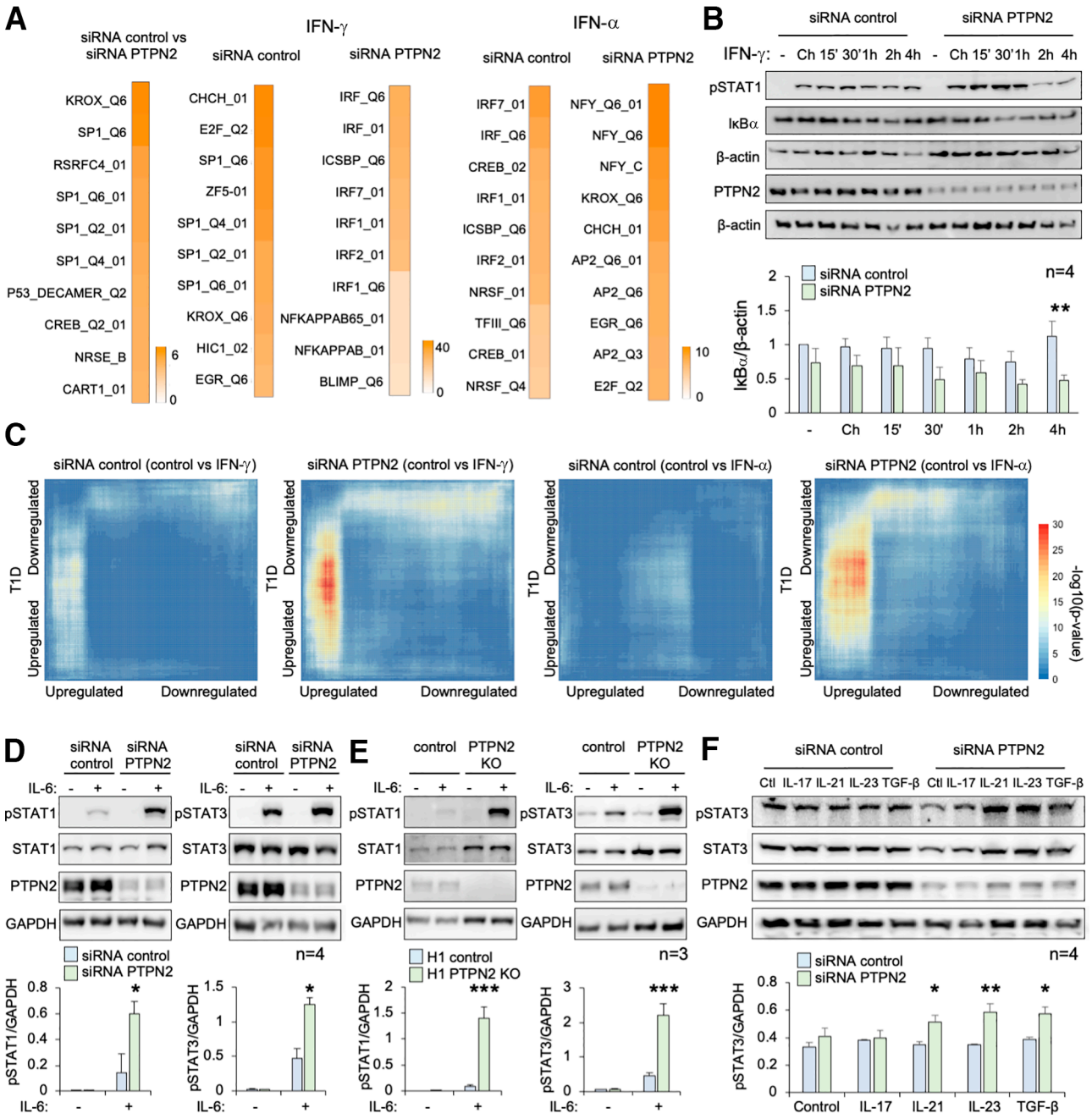

Figure 4—Gene modulation by PTPN2 under proinflammatory cytokine stimulation correlates with gene expression of primary β-cells from individuals with T1D. *A*: Modulated transcription factors regulated by PTPN2 and proinflammatory cytokine stimulation were predicted with use of the PASTAA software. The 10 most associated transcription factors are shown ($P < 0.05$). *B*: Transfected EndoC-βH1 cells with control or PTPN2 siRNA were cultured with IFN-γ for 1 h in a pulse-chase experiment. pSTAT1, IκBα, β-actin, PTPN2, and GAPDH were determined with Western blot. $n = 4$. *C*: RRHO comparison analysis was performed using RStudio as indicated. *D*: Transfected cells with control or PTPN2 siRNA were cultured with IL-6 for 1 h. Western blot for phosphorylated (p)STAT1/3, total STAT1/3, PTPN2, and GAPDH was performed. $n = 4$. *E*: hESC-derived β-like cells were cultured with IL-6 for 1 h. Western blot for phosphorylated STAT1/3, total STAT1/3, PTPN2, and GAPDH was performed. $n = 3$. *F*: Transfected EndoC-βH1 cells with control or PTPN2 siRNA were cultured with the proinflammatory cytokines as indicated for 1 h. Western blot for phosphorylated STAT3, total STAT3, PTPN2, and GAPDH was performed. $n = 4$. *$P < 0.05$; **$P < 0.01$; ***$P < 0.001$. Ctl, control.

siRNA control cells 24 h after the 1-h pulse with either IFN-γ or IFN-α and the data set of T1D β-cells (Fig. 4*C*). In contrast, we observed an overlap between gene profiles of PTPN2-deficient EndoC-βH1 cells exposed to IFN-γ or IFN-α and β-cells from individuals with T1D (Fig. 4*C*). In addition, PTPN2 deficiency in β-cells enhanced activation

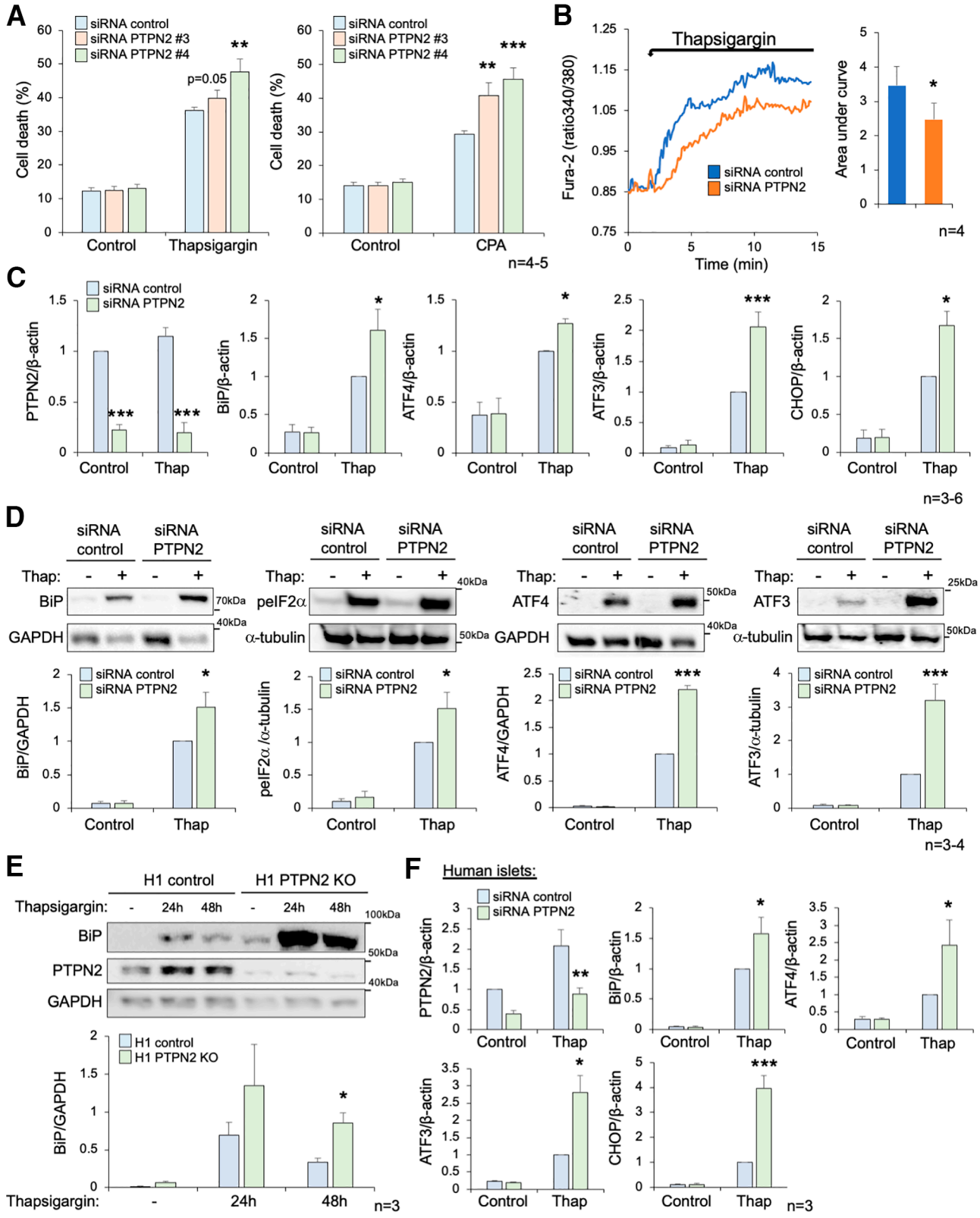

Figure 5—PTPN2 modulates ER stress–mediated cell death, ER stress marker expression, and Ca^{2+} intracellular levels in β-cells. *A*: Transfected EndoC-βH1 cells with control or two different PTPN2 siRNAs were treated with thapsigargin or CPA for 48 h. β-Cell apoptosis was evaluated by Hoechst 33342/propidium iodide staining. $n = 4–5$. *B*: Intracellular calcium levels were measured by Fura-2 dye in transfected EndoC-βH1 cells with PTPN2 or control siRNAs. Thapsigargin was added as indicated, and the area under the curve was measured. $n = 4$. ratio340/380, ratios of the 340- and 380-nm signals. *C*: Transfected EndoC-βH1 cells with PTPN2 or control siRNAs were cultured with thapsigargin (Thap) for 48 h. Gene expression of PTPN2 and ER stress markers was examined with qPCR. $n = 3–6$.

of additional cytokines involved in autoimmunity, i.e., IL-6, IL-21, IL-23, and TGF-β (47) (Fig. 4*D*–*F*). Overall, our results demonstrate a critical anti-inflammatory role of PTPN2 in the control of cytokine signaling in β-cells.

PTPN2 Deficiency Sensitizes β-Cells to Ca^{2+}-Dependent ER Stress

We observed increased PTPN2 and ER chaperone proteins in anti-CD3 + IL-1RA–treated NOD mice (Fig. 1) and modulation of unfolded protein response genes/ER stress by IFN-γ in PTPN2-deficient β-cells (Fig. 3*G*). A 48-kDa ER-located isoform of PTPN2 was previously identified (18), but its role in β-cells in autoimmune diabetes remains unknown. To determine whether PTPN2 regulates the unfolded protein response activation, we tested different chemical ER stressors. Interestingly, PTPN2 deficiency increased β-cell death induced by Ca^{2+}-dependent ER stress (thapsigargin and CPA) but did not impact tunicamycin toxicity induced by inhibition of the N-glycosylation in protein folding (Fig. 5*A* and Supplementary Fig. 14*A*). In line with these observations, PTPN2-deficient β-cells have reduced Ca^{2+} levels in the ER (Fig. 5*B*). The effect of PTPN2 inactivation in dysregulated Ca^{2+} homeostasis was not due to major changes in mRNA expression levels of the Ca^{2+} channels inositol triphosphate (IP_3), ryanodine receptor 2, the SERCA-2 pump, or the voltage-gated Ca^{2+} channels (Supplementary Fig. 14*B*). We detected BiP in the pull down of EndoC-βH1 overexpressing PTPN2, suggesting a direct protein-protein interaction (Supplementary Fig. 14*C*). PTPN2 knockdown enhanced mRNA and protein expression of ER stress markers in thapsigargin-treated EndoC-βH1 cells (Fig. 5*C* and *D*). Prolonged activation of the PERK/eIF2α/ATF4/Chop pathway results in cell death. Importantly, we confirmed our results in PTPN2 KO β-like cells and dispersed human islet cells transfected with PTPN2 siRNAs. Thus, thapsigargin increased ER stress–associated pathways in PTPN2-deficient cells (Fig. 5*E* and *F* and Supplementary Fig. 14*D*).

Ca^{2+} homeostasis is directly linked to membrane potential and β-cell function. Zero-current gramicidin-perforated patch-clamp voltage recordings were performed on insulin-producing H1 PTPN2 KO and control aggregates stimulated with 20 mmol/L glucose (Fig. 6*A*). H1 control cells displayed a limited electrical activity at 2.8 mmol/L glucose and it is increased after 20 mmol/L glucose stimulation, which approximates a normal β-cell response. Interestingly, the PTPN2 KO cells from aggregates constantly displayed a strong electrical activity at the different glucose concentrations (Fig. 6*A*), suggesting a dysregulated hyperactivation of the voltage-dependent Ca^{2+} and Na^{+} channels.

Next, we examined whether overexpression of different PTPN2 isoforms protects β-cells from dysregulated Ca^{2+}-induced ER stress and cell death. The 45-kDa or the 48-kDa PTPN2 isoforms were overexpressed using adenoviral vectors containing the human *PTPN2* cDNA under the control of the cytomegalovirus promoter. PTPN2 protein levels were efficiently increased in EndoC-βH1 at the different multiplicities of infection (Fig. 6*B* and Supplementary Fig. 15*A*). We selected multiplicity of infection 50 for subsequent experiments showing increased PTPN2 expression (Fig. 6*B* and *C*) and low toxicity (Supplementary Fig. 15*B*). The 45-kDa PTPN2 isoform abrogated IFN-γ–induced STAT1 phosphorylation (Supplementary Fig. 15*C*) but did not impact on Ca^{2+}-dependent ER stress–induced cell death (Supplementary Fig. 15*D*). The 48-kDa PTPN2 isoform decreased thapsigargin- and CPA-mediated cell death (Fig. 6*D* and *E*) but did not affect Ca^{2+}-independent ER stress toxicity induced by tunicamycin or brefeldin A (Supplementary Fig. 15*E*). Importantly, EndoC-βH1 cells transduced with 48 kDa AdPTPN2 decreased thapsigargin-induced caspase-3 activation and BiP protein expression (Fig. 6*F* and *G*). Taken together, our data show an isoform-dependent PTPN2 modulation of IFN-induced gene signaling and ER stress–mediated apoptosis in β-cells.

DISCUSSION

The ability to modulate selectively inflammatory signal transduction pathways holds therapeutic potential for T1D and other autoimmune disorders (48). In the current study, we established the capacity of PTPN2 to prevent inflammatory signaling and to positively modulate the Ca^{2+}-dependent unfolded protein response in pancreatic β-cells. In particular, we demonstrated that PTPN2 deficiency exacerbates both type I and type II IFN–dependent networks in β-cells and the potential progression toward autoimmunity. In addition, our study suggests that the localized activity of PTPN2, in concert with other protective pathways (7,8,29,49), can ameliorate the development of ER stress in β-cells.

The JAK/STAT signaling pathway induces immune-mediated β-cell dysfunction and death in T1D (5). We observed that PTPN2 deficiency in the β-cells resulted in increased STAT1 activation and downstream targets of type I and type II IFNs, in line with previous studies (17,38). We went beyond and provided a comprehensive gene network regulated by PTPN2 contributing to the amplification of the inflammatory response. There is a strong correlation between the levels of STAT1 measured

D: Transfected EndoC-βH1 cells with PTPN2 or control siRNAs were cultured with thapsigargin for 48 h. Protein expression of ER stress markers was examined with Western blot. $n = 3$–4. *E*: Dispersed H1-derived β-like cells were cultured with thapsigargin for 24 or 48 h as indicated. Protein expression of ER chaperone BiP was examined by Western blot. $n = 3$. *F*: Transfected dispersed human islets with PTPN2 or control siRNAs were cultured with thapsigargin for 24 h. Gene expression of PTPN2 and ER stress markers was examined with qPCR. $n = 3$. $^{*}P < 0.05$; $^{**}P < 0.01$; $^{***}P < 0.001$.

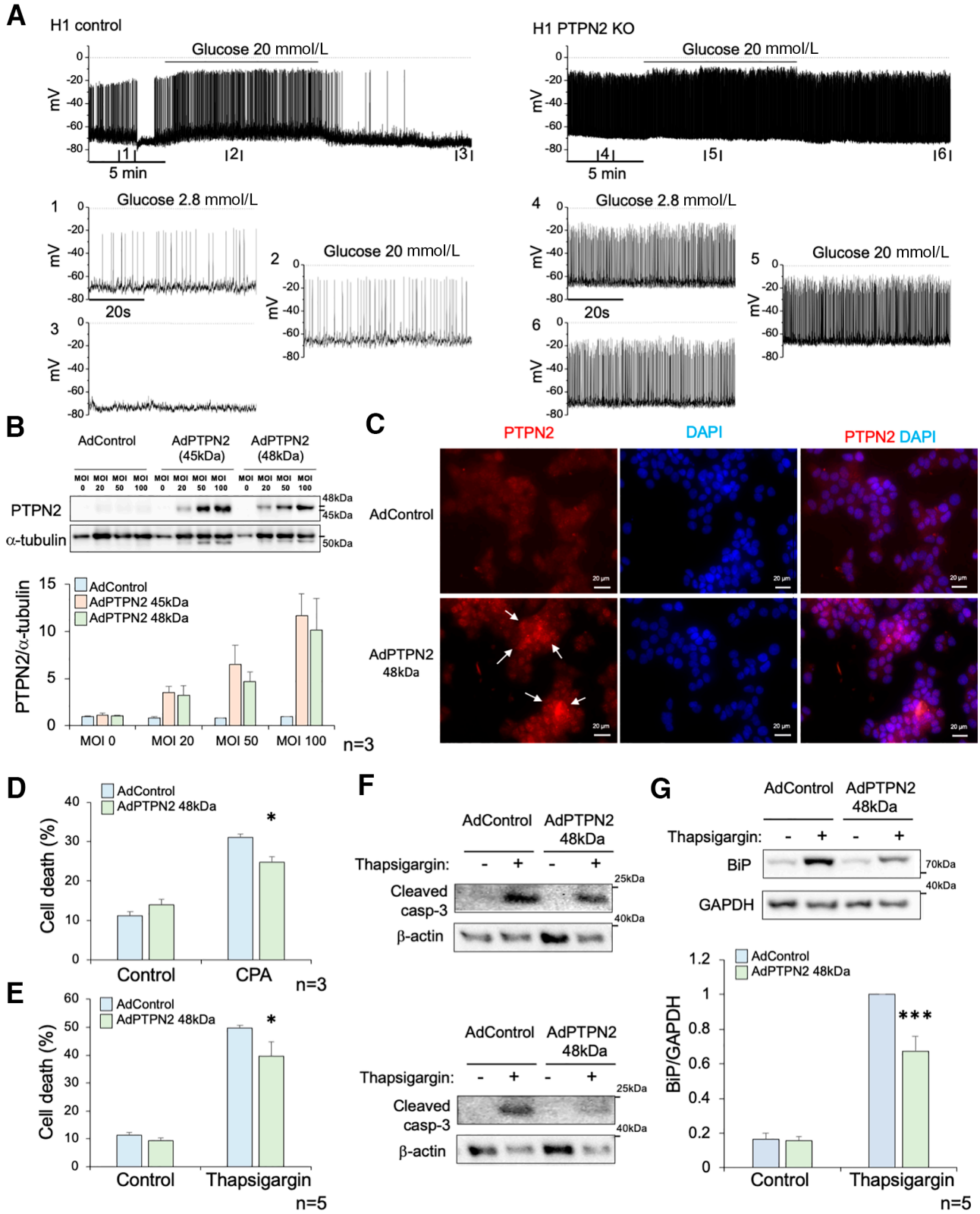

Figure 6—PTPN2 deficiency affects the membrane potential, and its overexpression ameliorates SERCA-mediated ER stress in β-cells. *A*: Zero-current gramicidin-perforated patch-clamp voltage recordings. Sampling rate: 5 kHz. Dotted lines represent zero-voltage level. 1–3: Glucose stimulated in differentiated H1 control aggregates (2.8 and 20 mmol/L glucose). 4–6: Glucose stimulated in differentiated H1 PTPN2 KO aggregates (2.8 and 20 mmol/L glucose). 1 and 4: Magnification of the electrical activity of the cells during min 3 with 2.8 mmol/L glucose in the bath medium. 2 and 5: Magnification of the electrical activity of the cells during min 10 with 20 mmol/L glucose in the bath medium. 3 and 6: Magnification of the electrical activity of the cells during min 25 with 2.8 mmol/L glucose in the bath medium

in the β-cells of patients with T1D and HLA-I hyperexpression, and the IFN gene signature (50). STAT1 deficiency in NOD mice prevents islet inflammation (51) and protects β-cells against immune-mediated destruction induced by multiple low doses of streptozotocin (52). Our results demonstrate that PTPN2 deficiency exacerbates STAT1 and other transcription factor activity, affecting approximately double the IFN-modulated gene inflammatory signature of β-cells. It is conceivable that β-cells with deficient PTPN2 activity are more susceptible to the autoimmune attack in T1D. In keeping with this, we demonstrated an association between gene expression induced by PTPN2 deficiency and IFN treatment in EndoC-βH1 cells and β-cells from individuals with T1D (46). Moreover, PTPN2 deficiency in β-cells also enhances STAT1/3 activation of IL-6, IL-21, IL-23, and TGF-β, proinflammatory cytokines involved in autoimmune diabetes (47).

It has been long known that insulin-producing β-cells have a developed ER and are consequently more prone to ER stress than nonsecretory cells (9,53). This susceptibility has been postulated as one of the initial mechanisms of β-cell dysfunction and death in early T1D (7,54). Thus, ER stress triggers β-cell dysfunction and apoptosis during inflammation (8,53). The unfolded protein response aims to alleviate ER stress by induction of transcription of genes linked to protein folding. We observed upregulation of BiP, GRP94, MANF, and PTPN2 in the pancreas/islets from anti-CD3 + IL-1RA–treated NOD mice. This eventually allows β-cells to maintain functionality and survive the autoimmune storm (49). PTPN2 was previously associated with ER stress regulation and β-cell function in obesity (55,56). We demonstrate that PTPN2 regulates the Ca^{2+}-dependent pathway of the unfolded protein response. PTPN2 deficiency affected inactivation of the SERCA pump leading to ER Ca^{2+} depletion (CPA and thapsigargin) but did not impact on inhibition of N-linked protein glycosylation in the ER (tunicamycin) or inhibition of vesicle formation and transport between the ER and the Golgi apparatus (brefeldin A), suggesting specificity of PTPN2 activity at the ER. High levels of ER Ca^{2+} are required to promote proper protein folding (57), as ER resident chaperones have Ca^{2+}-dependent regulatory motifs. We postulate that PTPN2 deficiency induces Ca^{2+} leak at the ER sensitizing β-cells to hyperactivation of the PERK/eIF2α/ATF4/Chop pathway. BiP is a major ER chaperone protein and has a role in binding Ca^{2+} to buffer ∼25% of the luminal Ca^{2+} load (57). PTPN2 regulates and directly binds to BiP in β-cells (present data). BiP expression was upregulated by PTPN2 deficiency and attenuated by PTPN2 overexpression in β-cells exposed to SERCA blockers. Interestingly, BiP posttranslational modifications are associated with antigen presentation and the autoimmune process (58).

PTPN2 expression in the pancreas correlated positively with anti-CD3 + IL-1RA therapy outcome in a small cohort of NOD mice. We did not observe diabetes remission in anti-CD3–treated mice. This is probably due to the low concentration of anti-CD3 mAb and the number of mice used in our study. It is expected that in large cohorts, a percentage of mice can be cured with the monotherapies (19), and PTP/protein expression should be analyzed in the different subgroups. In addition, measurements of PTPN2/chaperone mRNA and protein expression at different time points in large cohorts of β-cell–specific PTPN2 knockout/wild-type NOD mice will be required to gain additional in vivo mechanistic insight. This is beyond the scope of the present work. Although in this study we focused our attention on the role of PTPN2 in the β-cells and islets, it is conceivable that PTPN2 in immune cells also contributes to the amelioration of the inflammatory process of autoimmune diabetes. Consistent with this, $CD8^+$ T cells lacking PTPN2 and cross primed by β-cell self-antigens escape tolerance and acquire cytotoxic T cell activity, resulting in β-cell destruction in the RIP-mOVA mouse model of autoimmune diabetes (59). Moreover, T cell PTPN2 deficiency in NOD mice accelerated the onset and increased the incidence of diabetes (60). Additional work is required to determine whether overexpression of PTPN2 in immune cells or β-cells can prevent or reverse the development of autoimmune diabetes in patients. Importantly, we have demonstrated that our proteomic approach can be integrated in future studies to determine protein expression and PTP levels in pancreatic cells in T1D samples.

In conclusion, we demonstrate that PTPN2 plays a key anti-inflammatory role in β-cell dysfunction in the context of IFN signaling and ER stress. PTPN2 deficiency can light up the "danger signal" in early T1D and, together with the local amplification of proinflammatory cytokines and chemokines, activate the expansion of the autoimmune cells. Our findings provide fundamental evidence that PTPN2 is an important regulator of β-cell inflammation and

after the 20 mmol/L glucose stimulation. Measurement representative of two independent experiments. *B*: EndoC-βH1 cells were transduced with inactive adenovirus (AdControl), AdPTPN2 45 kDa, or AdPTPN2 48 kDa. The relative protein expression of the PTPN2 was determined with Western blot 72 h after transduction. $n = 3$. *C*: Immunofluorescence staining of PTPN2 in EndoC-βH1 cells transduced with AdPTPN2 48 kDa or AdControl. PTPN2 overexpression in AdPTPN2 48 kDa is shown (white arrows). The nuclei were visualized with DAPI. Scale bar: 20 μm. *D*: Transduced cells with AdPTPN2 48 kDa or AdControl were cultured with CPA for 48 h. β-Cell apoptosis was evaluated with Hoechst 33342/propidium iodide staining. $n = 3$. *E–G*: Transduced cells with AdPTPN2 48 kDa or AdControl were cultured with thapsigargin for 48 h. *E*: β-Cell apoptosis was evaluated with Hoechst 33342/propidium iodide staining. $n = 5$. *F*: Cleaved caspase-3 activation was evaluated with Western blot in cells transduced with AdPTPN2 48 kDa or AdControl and treated with thapsigargin for 48 h as indicated. $n = 2$. *G*: Transduced cells with AdPTPN2 48 kDa or AdControl were cultured with thapsigargin for 48 h. Expression of ER stress marker BiP was examined by Western blot. $n = 5$. $^*P < 0.05$; $^{**}P < 0.01$; $^{***}P < 0.001$.

support the active role of β-cells in their own demise in T1D.

Acknowledgments. The authors thank Madalina Popa, André Dias, Grégory Vegh, personnel from the ULB Center for Diabetes Research (Université Libre de Bruxelles), and Marijke Viaene (Katholieke Universiteit Leuven) for experimental and technical support; Alessandra K. Cardozo (Université Libre de Bruxelles) for critical reading of the manuscript; and Piero Marchetti and the Pancreatic Islet Laboratory in Pisa (University of Pisa) for human islets.

Funding. This work was supported by a Fonds National de la Recherche Scientifique (FNRS)-MIS grant (33650793), European Research Council Consolidator grant METAPTPs (GA817940), and a JDRF Career Development Award (CDA-2019-758-A-N). B.E. and V.V. are supported by an FNRS CR postdoctoral fellowship (34769436) and PhD Aspirant scholarship, respectively. S.P.S. is supported by mandat d'impulsion scientifique - mobilité Ulysse (MISU) funding from the FNRS (34772792 [SCHISM]). E.N.G. is a Research Associate of the FNRS (Brussels, Belgium).

Duality of Interest. No potential conflicts of interest relevant to this article were reported.

Author Contributions. B.E., V.V., J.B.-M., R.C., J.N., H.I., M.L.W., M.K.B., B.V., and P.-J.M. researched data and reviewed and edited the manuscript. S.P.S. and F.R. contributed to data analysis. P.L., T.O., C.G., and W.W. contributed to research data and experimental design and reviewed and edited the manuscript. E.N.G. researched data, contributed to designed experiments, and reviewed, edited, and wrote the manuscript. E.N.G. is the guarantor of this work and, as such, had full access to all the data in the study and takes responsibility for the integrity of the data and the accuracy of the data analysis.

References

1. Christoffersson G, Rodriguez-Calvo T, von Herrath M. Recent advances in understanding type 1 diabetes. F1000 Res 2016;5:F1000 Faculty Rev-110
2. Claessens LA, Wesselius J, van Lummel M, et al. Clinical and genetic correlates of islet-autoimmune signatures in juvenile-onset type 1 diabetes. Diabetologia 2020;63:351–361
3. Bender C, Rodriguez-Calvo T, Amirian N, Coppieters KT, von Herrath MG. The healthy exocrine pancreas contains preproinsulin-specific CD8 T cells that attack islets in type 1 diabetes. Sci Adv 2020;6:eabc5586
4. Roep BO, Thomaidou S, van Tienhoven R, Zaldumbide A. Type 1 diabetes mellitus as a disease of the β-cell (do not blame the immune system?). Nat Rev Endocrinol 2021;17:150–161
5. Gurzov EN, Stanley WJ, Pappas EG, Thomas HE, Gough DJ. The JAK/STAT pathway in obesity and diabetes. FEBS J 2016;283:3002–3015
6. Huang X, Yuang J, Goddard A, et al. Interferon expression in the pancreases of patients with type I diabetes. Diabetes 1995;44:658–664
7. Clark AL, Urano F. Endoplasmic reticulum stress in beta cells and autoimmune diabetes. Curr Opin Immunol 2016;43:60–66
8. Gurzov EN, Eizirik DL. Bcl-2 proteins in diabetes: mitochondrial pathways of β-cell death and dysfunction. Trends Cell Biol 2011;21:424–431
9. Cardozo AK, Ortis F, Storling J, et al. Cytokines downregulate the sarcoendoplasmic reticulum pump Ca2+ ATPase 2b and deplete endoplasmic reticulum Ca2+, leading to induction of endoplasmic reticulum stress in pancreatic beta-cells. Diabetes 2005;54:452–461
10. Thomaidou S, Zaldumbide A, Roep BO. Islet stress, degradation and autoimmunity. Diabetes Obes Metab 2018;20(Suppl. 2):88–94
11. Gurzov EN, Stanley WJ, Brodnicki TC, Thomas HE. Protein tyrosine phosphatases: molecular switches in metabolism and diabetes. Trends Endocrinol Metab 2015;26:30–39
12. Barrett JC, Clayton DG, Concannon P, et al.; Type 1 Diabetes Genetics Consortium. Genome-wide association study and meta-analysis find that over 40 loci affect risk of type 1 diabetes. Nat Genet 2009;41:703–707
13. Espino-Paisan L, de la Calle H, Fernández-Arquero M, et al. A polymorphism in PTPN2 gene is associated with an earlier onset of type 1 diabetes. Immunogenetics 2011;63:255–258
14. Bieschke J, Herbst M, Wiglenda T, et al. Small-molecule conversion of toxic oligomers to nontoxic β-sheet-rich amyloid fibrils. Nat Chem Biol 2011;8:93–101
15. Okuno M, Ayabe T, Yokota I, et al.; Japanese Study Group of Insulin Therapy for Childhood and Adolescent Diabetes. Protein-altering variants of PTPN2 in childhood-onset Type 1A diabetes. Diabet Med 2018;35:376–380
16. Stanley WJ, Litwak SA, Quah HS, et al. Inactivation of protein tyrosine phosphatases enhances interferon signaling in pancreatic islets. Diabetes 2015;64:2489–2496
17. Santin I, Moore F, Colli ML, et al. PTPN2, a candidate gene for type 1 diabetes, modulates pancreatic β-cell apoptosis via regulation of the BH3-only protein Bim. Diabetes 2011;60:3279–3288
18. ten Hoeve J, de Jesus Ibarra-Sanchez M, Fu Y, et al. Identification of a nuclear Stat1 protein tyrosine phosphatase. Mol Cell Biol 2002;22:5662–5668
19. Takiishi T, Korf H, Van Belle TL, et al. Reversal of autoimmune diabetes by restoration of antigen-specific tolerance using genetically modified Lactococcus lactis in mice. J Clin Invest 2012;122:1717–1725
20. Gurzov EN, Barthson J, Marhfour I, et al. Pancreatic β-cells activate a JunB/ATF3-dependent survival pathway during inflammation. Oncogene 2012;31:1723–1732
21. Trokovic R, Weltner J, Noisa P, Raivio T, Otonkoski T. Combined negative effect of donor age and time in culture on the reprogramming efficiency into induced pluripotent stem cells. Stem Cell Res (Amst) 2015;15:254–262
22. Achuta VS, Grym H, Putkonen N, et al. Metabotropic glutamate receptor 5 responses dictate differentiation of neural progenitors to NMDA-responsive cells in fragile X syndrome. Dev Neurobiol 2017;77:438–453
23. Saarimäki-Vire J, Balboa D, Russell MA, et al. An activating STAT3 mutation causes neonatal diabetes through premature induction of pancreatic differentiation. Cell Rep 2017;19:281–294
24. Pagliuca FW, Millman JR, Gürtler M, et al. Generation of functional human pancreatic β cells in vitro. Cell 2014;159:428–439
25. Rezania A, Bruin JE, Arora P, et al. Reversal of diabetes with insulin-producing cells derived in vitro from human pluripotent stem cells. Nat Biotechnol 2014;32:1121–1133
26. Ravassard P, Hazhouz Y, Pechberty S, et al. A genetically engineered human pancreatic β cell line exhibiting glucose-inducible insulin secretion. J Clin Invest 2011;121:3589–3597
27. Schaschkow A, Pang L, Vandenbempt V, et al. STAT3 regulates mitochondrial gene expression in pancreatic β-cells and its deficiency induces glucose intolerance in obesity. Diabetes 2021;70:2026–2041
28. Meyerovich K, Violato NM, Fukaya M, et al. MCL-1 is a key antiapoptotic protein in human and rodent pancreatic β-cells. Diabetes 2017;66:2446–2458
29. Gurzov EN, Ortis F, Cunha DA, et al. Signaling by IL-1beta+IFN-gamma and ER stress converge on DP5/Hrk activation: a novel mechanism for pancreatic beta-cell apoptosis. Cell Death Differ 2009;16:1539–1550
30. Wu W, Hale AJ, Lemeer S, den Hertog J. Differential oxidation of protein-tyrosine phosphatases during zebrafish caudal fin regeneration. Sci Rep 2017;7:8460
31. Gurzov EN, Tran M, Fernandez-Rojo MA, et al. Hepatic oxidative stress promotes insulin-STAT-5 signaling and obesity by inactivating protein tyrosine phosphatase N2. Cell Metab 2014;20:85–102
32. Litwak SA, Wali JA, Pappas EG, et al. Lipotoxic stress induces pancreatic β-cell apoptosis through modulation of Bcl-2 proteins by the ubiquitin-proteasome system. J Diabetes Res 2015;2015:280615

33. Roider HG, Manke T, O'Keeffe S, Vingron M, Haas SA. PASTAA: identifying transcription factors associated with sets of co-regulated genes. Bioinformatics 2009;25:435–442
34. Van Eylen F, Lebeau C, Albuquerque-Silva J, Herchuelz A. Contribution of Na/Ca exchange to Ca2+ outflow and entry in the rat pancreatic beta-cell: studies with antisense oligonucleotides. Diabetes 1998;47:1873–1880
35. Crutzen R, Virreira M, Markadieu N, et al. Anoctamin 1 (Ano1) is required for glucose-induced membrane potential oscillations and insulin secretion by murine β-cells. Pflugers Arch 2016;468:573–591
36. Ablamunits V, Henegariu O, Hansen JB, et al. Synergistic reversal of type 1 diabetes in NOD mice with anti-CD3 and interleukin-1 blockade: evidence of improved immune regulation. Diabetes 2012;61:145–154
37. Gump JM, Staskiewicz L, Morgan MJ, Bamberg A, Riches DW, Thorburn A. Autophagy variation within a cell population determines cell fate through selective degradation of Fap-1. Nat Cell Biol 2014;16:47–54
38. Moore F, Colli ML, Cnop M, et al. PTPN2, a candidate gene for type 1 diabetes, modulates interferon-gamma-induced pancreatic beta-cell apoptosis. Diabetes 2009;58:1283–1291
39. Qing Y, Stark GR. Alternative activation of STAT1 and STAT3 in response to interferon-gamma. J Biol Chem 2004;279:41679–41685
40. Foulis AK, Farquharson MA, Meager A. Immunoreactive alpha-interferon in insulin-secreting beta cells in type 1 diabetes mellitus. Lancet 1987; 2:1423–1427
41. Ferreira RC, Guo H, Coulson RM, et al. A type I interferon transcriptional signature precedes autoimmunity in children genetically at risk for type 1 diabetes. Diabetes 2014;63:2538–2550
42. Carrero JA, Benshoff ND, Nalley K, Unanue ER. Type I and II interferon receptors differentially regulate type 1 diabetes susceptibility in male versus female NOD mice. Diabetes 2018;67:1830–1835
43. Moore F, Naamane N, Colli ML, et al. STAT1 is a master regulator of pancreatic beta-cell apoptosis and islet inflammation. J Biol Chem 2011; 286:929–941
44. Sachini N, Papamatheakis J. NF-Y and the immune response: dissecting the complex regulation of MHC genes. Biochim Biophys Acta Gene Regul Mech 2017;1860:537–542
45. Plaisier SB, Taschereau R, Wong JA, Graeber TG. Rank-rank hypergeometric overlap: identification of statistically significant overlap between gene-expression signatures. Nucleic Acids Res 2010;38:e169
46. Russell MA, Redick SD, Blodgett DM, et al. HLA class II antigen processing and presentation pathway components demonstrated by transcriptome and protein analyses of islet β-cells from donors with type 1 diabetes. Diabetes 2019;68:988–1001
47. Clark M, Kroger CJ, Tisch RM. Type 1 diabetes: a chronic anti-self-inflammatory response. Front Immunol 2017;8:1898
48. Gurzov EN, Ke PC, Ahlgren U, Garcia Ribeiro RS, Gotthardt M. Novel strategies to protect and visualize pancreatic β cells in diabetes. Trends Endocrinol Metab 2020;31:905–917
49. Engin F, Yermalovich A, Nguyen T, et al. Restoration of the unfolded protein response in pancreatic β cells protects mice against type 1 diabetes. Sci Transl Med 2013;5:211ra156
50. Richardson SJ, Rodriguez-Calvo T, Gerling IC, et al. Islet cell hyperexpression of HLA class I antigens: a defining feature in type 1 diabetes. Diabetologia 2016;59:2448–2458
51. Kim S, Kim HS, Chung KW, et al. Essential role for signal transducer and activator of transcription-1 in pancreatic beta-cell death and autoimmune type 1 diabetes of nonobese diabetic mice. Diabetes 2007;56:2561–2568
52. Gysemans CA, Ladrière L, Callewaert H, et al. Disruption of the gamma-interferon signaling pathway at the level of signal transducer and activator of transcription-1 prevents immune destruction of beta-cells. Diabetes 2005; 54:2396–2403
53. Scheuner D, Kaufman RJ. The unfolded protein response: a pathway that links insulin demand with beta-cell failure and diabetes. Endocr Rev 2008; 29:317–333
54. Tersey SA, Nishiki Y, Templin AT, et al. Islet β-cell endoplasmic reticulum stress precedes the onset of type 1 diabetes in the nonobese diabetic mouse model. Diabetes 2012;61:818–827
55. Bettaieb A, Liu S, Xi Y, et al. Differential regulation of endoplasmic reticulum stress by protein tyrosine phosphatase 1B and T cell protein tyrosine phosphatase. J Biol Chem 2011;286:9225–9235
56. Xi Y, Liu S, Bettaieb A, et al. Pancreatic T cell protein-tyrosine phosphatase deficiency affects beta cell function in mice. Diabetologia 2015;58:122–131
57. Preissler S, Rato C, Yan Y, Perera LA, Czako A, Ron D. Calcium depletion challenges endoplasmic reticulum proteostasis by destabilising BiP-substrate complexes. eLife 2020;9:e62601
58. Buitinga M, Callebaut A, Marques Câmara Sodré F, et al. Inflammation-induced citrullinated glucose-regulated protein 78 elicits immune responses in human type 1 diabetes. Diabetes 2018;67:2337–2348
59. Wiede F, Ziegler A, Zehn D, Tiganis T. PTPN2 restrains CD8+ T cell responses after antigen cross-presentation for the maintenance of peripheral tolerance in mice. J Autoimmun 2014;53:105–114
60. Wiede F, Brodnicki TC, Goh PK, et al. T-cell-specific PTPN2 deficiency in NOD mice accelerates the development of type 1 diabetes and autoimmune comorbidities. Diabetes 2019;68:1251–1266